Inorganic Chemistry

Article

pubs.acs.org/IC

# Synthesis and Structural Studies of Diorganotin(IV)-Based Coordination Polymers Bearing Silaalkylphosphonate Ligands and Their Transformation into Colloidal Domains

Ravi Shankar,*[,†] Nisha Singla,[†] Meenal Asija,[†] Gabriele Kociok-Köhn,[‡] and Kieran C. Molloy[‡]

[†]Department of Chemistry, Indian Institute of Technology, Hauz Khas, New Delhi 110016, India

[‡]Department of Chemistry, University of Bath, Bath BA2 7AY, U.K.

Supporting Information

**ABSTRACT:** The contribution of silaalkylphosphonic acids $Me_3SiCH_2P(O)(OH)_2$ (**1**) and $Me_3SiC(CH_3)_2P(O)(OH)_2$ (**2**) as ligands was demonstrated for the first time by the isolation of new diorganotin(IV) phosphonates $Et_2Sn\{OP(O)(OH)CH_2SiMe_3\}(OSO_2Me)$ (**3**), $(Et_2Sn)_6\{O_3PC(CH_3)_2SiMe_3\}_4(OSO_2Me)_4$ (**4**), and $Et_2Sn(O_3PCH_2SiMe_3)$ (**5**). X-ray crystallographic studies of **1**−**4** are presented. The structures of **1** and **2** adopt extended motifs by virtue of P−OH···O═P-type hydrogen bonding interactions. The molecular structure of **3** is composed of a dimer formed by bridging hydrogen phosphonate groups, while the sulfonate group appended on each tin atom acts in a $\mu_2$-bridging mode to afford the formation of one-dimensional coordination polymer featuring alternate eight-membered $[-Sn-O-P-O-]_2$ and $[-Sn-O-S-O-]_2$ rings. The asymmetric unit of **4** is composed of two crystallographically unique trinuclear tin phosphonate clusters with a $Sn_3(\mu_3\text{-}PO_3)_2$ core linked together by coordinative association of a $\mu_2$-sulfonate group, while the remaining sulfonates are involved in the construction of a two-dimensional self-assembly. The identity of **1**−**5** in solution was established by IR and multinuclear ($^1H$, $^{13}C$, $^{31}P$, $^{119}Sn$) NMR spectroscopy. The presence of silaalkyl group in **5** imparts unusual solubility in hydrocarbon, aromatic, and ether solvents. As a consequence, the formation of colloidal particles of **5** featuring rodlike morphology was achieved by ultrasonication of a solution in ethanol−chloroform mixture.

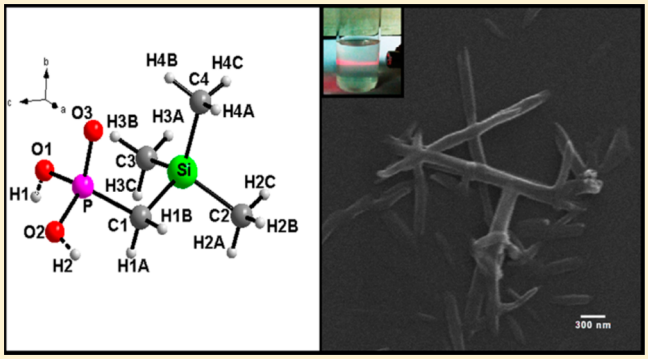


## INTRODUCTION

The contribution of phosphonate ligands in both monoanionic $[RP(O)(OH)O]^-$ and dianionic $[RPO_3]^{2-}$ forms has been well-recognized in the construction of organotin(IV) phosphonates featuring structurally variable coordination frameworks ranging from cluster entities to two-/three-dimensional (2D/3D) polymeric motifs. Among the known examples of organotin clusters,[1] the skeletal framework is often composed of oxo-/hydroxotin species as the constructing units bearing phosphonate groups as the complexing ligand. The structure of $Bu_2Sn\{OP(O)(OH)Me\}_2$ in the solid state is best described as a one-dimensional (1D) polymer resulting from strong and weak Sn ← O contacts [Sn−O = 2.165, 3.18 Å] of the hydrogen phosphonate ligands,[2] while $Me_3Sn\{OP(O)(OH)Ph\}$ adopts a helical polymeric motif.[3] The contribution of tridentate $[RPO_3]^{2-}$ ligand has been exemplified in *n*-$Bu_2Sn(O_3PPh)$, $(Me_3Sn)_4(O_3PPh)_2$, and $(Me_3Sn)_2(O_3PPh)$. MeOH and $Me_2Sn(O_3PPh)$, wherein formation of 1D/2D polymeric structures are particularly noticeable.[4] The complex $Ph_3Sn\{OP(O)(OMe)Me\}$, derived from phosphonate ester, is a unique example of a cyclic hexamer with five-coordinated tin atoms.[5] The synthesis and structural chemistry of several organotin(IV) phosphonate diesters as molecular entities has been reported.[6] These studies have provided a great deal of insight into the reactivity behavior of these complexes both at metal and the ligand centers. The contribution in this area from our group relates to synthesis and structural characterization of several mixed-ligand diorganotin(IV) coordination polymers of general composition $R_2Sn\{OP(O)(OH)R^1\}(OSO_2R^2)$ and $(R_2Sn)_3(O_3PR^1)_2(OSO_2R^2)_2$ (R = Me, Et, *n*-Bu; $R^1$, $R^2$ = alkyl or Ph). Among these families, incorporation of sulfonate groups as the appended donor functionality on tin-phosphonate framework and its ubiquitous ($\mu_2$, $\mu_3$) bonding affinity toward tin has opened up interesting opportunities to construct novel structural motifs.[7]

In recent years, there have been persistent efforts directed toward evolving synthetic methods to transform infinite coordination polymers (ICPs) into nano/colloidal size domains and unfolding their promising applications in catalysis, gas sorption, biomedical imaging, biosensing, etc.[8] To this end, transition metal based 1D and layered coordination frameworks

**Received:** March 25, 2014
**Published:** May 22, 2014

   dx.doi.org/10.1021/ic500682t | *Inorg. Chem.* 2014, 53, 6195−6203

Table 1. Summary of Crystallographic Data for 1−4

| crystal data | 1 | 2 | 3 | 4 |
|---|---|---|---|---|
| empirical formula | $C_4H_{13}O_3PSi$ | $C_6H_{17}O_3PSi$ | $C_9H_{25}O_6PSSiSn$ | $C_{52}H_{132}O_{24}P_4S_4Si_4O_6$ |
| fw | 168.20 | 196.25 | 439.10 | 2218.19 |
| temperature (K) | 150(2) | 150(2) | 150(2) | 150(2) |
| wavelength (Å) | 0.710 73 | 0.710 73 | 0.710 73 | 0.710 73 |
| cryst syst | orthorhombic | orthorhombic | triclinic | monoclinic |
| space group | $P2_12_12_1$ | *Pnab* | $P\bar{1}$ | $P2_1/n$ |
| *a*, Å | 6.1752(2) | 10.6670(2) | 8.6436(3) | 21.5869(3) |
| *b*, Å | 6.6929(2) | 13.0947(3) | 10.3127(3) | 19.7660(3) |
| *c*, Å | 21.5021(6) | 14.9488(3) | 12.1930(4) | 21.8682(3) |
| *α*, deg | 90 | 90 | 67.8301(13) | 90 |
| *β*, deg | 90 | 90 | 87.0945(14) | 104.8080(10) |
| *γ*, deg | 90 | 90 | 66.139(2) | 90 |
| *V*, Å$^3$ | 888.68(5) | 2088.07(7) | 913.79(5) | 9021.0(2) |
| *Z* | 4 | 8 | 2 | 4 |
| *ρ* calcd. (Mg/m$^3$) | 1.257 | 1.249 | 1.596 | 1.633 |
| *μ* (mm$^{-1}$) | 0.392 | 0.344 | 1.680 | 1.912 |
| *F*(000) | 360 | 848 | 444 | 4464 |
| crystal size (mm$^3$) | 0.300 × 0.200 × 0.150 | 0.200 × 0.150 × 0.150 | 0.200 × 0.150 × 0.150 | 0.250 × 0.200 × 0.200 |
| *θ* (deg) | 3.433 to 27.519 | 3.651 to 27.461 | 2.984 to 27.581 | 3.551 to 27.334 |
| reflns colld | 14 469 | 27 912 | 15 658 | 86 132 |
| unique reflens | 2032 | 2385 | 4113 | 19 598 |
| completeness to *θ* | 25.242° (99.3%) | 25.242° (99.6%) | 25.242° (99.1%) | 25.242° (96.6%) |
| max. and min. transmn. | 0.946 and 0.853 | 0.954 and 0.866 | 0.732 and 0.782 | 0.859 and 0.797 |
| *R*(int) | 0.0661 | 0.0630 | 0.0326 | 0.0835 |
| data/restraints/parameters | 2032/1/93 | 2385/0/113 | 4113/1/182 | 19598/6/933 |
| GOF on $F^2$ | 1.093 | 1.099 | 1.079 | 1.041 |
| final *R* indices [$I > 2\sigma(I)$] | *R*1 = 0.0272, *wR*2 = 0.0618 | *R*1 = 0.0345, *wR*2 = 0.0832 | *R*1 = 0.0254, *wR*2 = 0.0563 | *R*1 = 0.0370, *wR*2 = 0.078 |
| *R* indices (all data) | *R*1 = 0.0297, *wR*2 = 0.0633 | *R*1 = 0.0448, *wR*2 = 0.0888 | *R*1 = 0.0292, *wR*2 = 0.0581 | *R*1 = 0.0622, *wR*2 = 0.088 |
| absolute structure parameter | 0.00(5) | | | |
| largest diff. peak and hole (e Å$^{-3}$) | 0.305 and −0.260 | 0.287 and −0.304 | 0.727 and −0.976 | 0.855 and −1.036 |

that exhibit weak noncovalent interactions in the solid state are particularly attractive candidates, as these interactions can be depleted in the presence of an external stimuli via a wet chemical approach and facilitate the formation of nanorods/nanowires[9] and nanosheets.[10] Among the metal-phosphonate family, realization of nano structures, however, still remains a formidable challenge in view of their tendency to form densely packed solid phases. The added complexity arising from their insoluble nature restricts structure tailorability by a wet chemical method. Maeda et al. have recently described the synthesis of a lanthanum−organophosphonate nanosheet by exfoliation of the layered structure derived from 1,3,5-benzenetriphosphonate ligand.[11] Several layered tin(IV) phosphonates, $Sn(O_3PR)_2$ and $Sn(O_3PRPO_3)$ (R = alkyl or aryl), have been synthesized by solvothermal approach and are known to exhibit porous characteristics as a result of aggregation of nanosized particles.[12]

To broaden the scope of organotin(IV) phosphonates in the development of nano-structured materials, we focused our attention to explore the potential of silaalkylphosphonic acids as ligands. It is important to emphasize that coordination chemistry of these ligands still remains in a state of dormancy despite a few early reports on the synthesis of sila-substituted phosphonic acids.[13] As part of our ongoing interest in metal coordination frameworks derived from oxyphosphorus-based ligands,[7,14] we surmised that incorporation of these ligands in the coordination assemblies might offer a possibility to modulate structural motifs as a result of steric and electronic attributes of silaalkyl groups. Herein we report a detailed study on the synthesis and structural aspects of two new silaalkylphosphonic acids, namely, $Me_3SiCR_2P(O)(OH)_2$ [R = H (**1**), $CH_3$ (**2**)] and diorganotin(IV) coordination polymers $Et_2Sn\{OP(O)(OH)CH_2SiMe_3\}(OSO_2Me)$ (**3**), $(Et_2Sn)_6\{O_3PC(CH_3)_2SiMe_3\}_4(OSO_2Me)_4$ (**4**), and $Et_2Sn(O_3PCH_2SiMe_3)$ (**5**) derived therefrom. Interestingly, introduction of the silaalkyl group in **5** imparts unusual solubility in hydrocarbon, aromatic, and ether solvents and facilitates the formation of colloidal particles with rodlike morphology.

## RESULTS AND DISCUSSION

### Synthesis and Characterization of Phosphonic Acids.

As a prerequisite, the synthesis of diethyltrimethylsilylmethylphosphonate, $Me_3SiCH_2P(O)(OEt)_2$ (**1a**), was achieved by following the procedure reported by Eaborn et al.[13a] The reaction involves Arbuzov rearrangement in triethylphosphite in the presence of (chloromethyl)trimethylsilane.

$$Me_3SiCH_2Cl + P(OEt)_3 \xrightarrow[140-150\,^\circ C]{N_2} \underset{(\mathbf{1a})}{Me_3SiCH_2P(O)(OEt)_2} + C_2H_5Cl$$

The active methylene group adjacent to silicon in **1a** undergoes deprotonation in the presence of a strong base such as *n*-butyl lithium in tetrahydrofuran (THF) at −60 °C, and subsequent addition of methyl iodide affords the formation of diethyl(2-trimethylsilyl)-2-propylphosphonate, $Me_3SiC(CH_3)_2P(O)$-


dx.doi.org/10.1021/ic500682t | Inorg. Chem. 2014, 53, 6195−6203

**Table 2. Selected Bond Lengths (Å) and Angles (deg) of 1**

| | | | |
|---|---|---|---|
| Si–C(3) | 1.859(2) | Si–C(2) | 1.863(2) |
| Si–C(4) | 1.869(3) | Si–C(1) | 1.8916(18) |
| P–O(3) | 1.5060(13) | P–O (2) | 1.5574(15) |
| P–O(1) | 1.5544(12) | P–C(1) | 1.7708(17) |
| O1–H1 | 0.90(2) | O2–H2 | 0.83(3) |
| P–C(1)–Si | 118.50(10) | | |
| O(1)–H(1)···O(3)[a] | 2.5579(19) | O(2)–H(2)···O(3)[b] | 2.5910(19) |

[a]Symmetry transformations used to generate equivalent atoms: $-x + 1, y - 1/2, -z + 1/2$. [b]Symmetry transformations used to generate equivalent atoms: $-x, y - 1/2, -z + 1/2$.

**Table 3. Selected Bond Lengths (Å) and Angles (deg) of 2**

| | | | |
|---|---|---|---|
| Si–C (3) | 1.859(2) | Si–C(2) | 1.859(2) |
| Si–C (4) | 1.9226(16) | Si–C(1) | 1.861(2) |
| P–O(3) | 1.5682(12) | P–O (2) | 1.5543(12) |
| P–O(1) | 1.5108(11) | P–C(4) | 1.7864(16) |
| O2–H1 | 0.81(3) | O3–H2 | 0.83(2) |
| P–C(4)–Si | 112.63(8) | | |
| O(2)–H(1)···O(1)[a] | 2.5771(17) | O(2)–H(2)···O(3)[b] | 2.6346(16) |

[a]Symmetry transformations used to generate equivalent atoms: $-x + 3/2, y, -z + 1$. [b]Symmetry transformations used to generate equivalent atoms: $-x + 1, -y, -z + 1$.

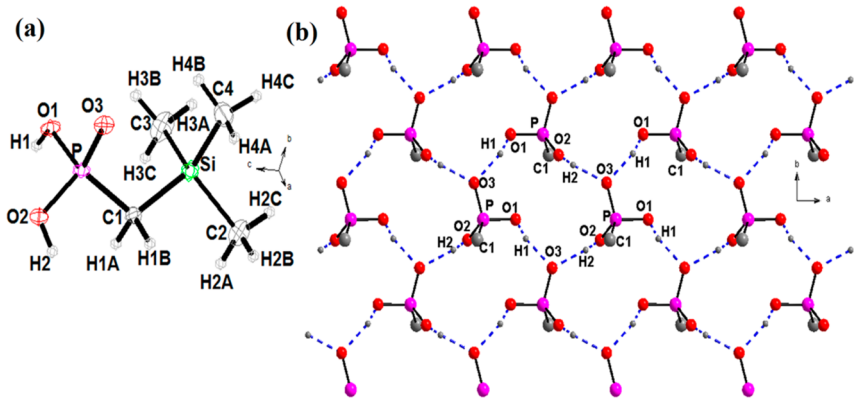


**Figure 1.** (a) ORTEP view of asymmetric unit of **1**. The thermal ellipsoids are set at 40% probability. (b) 2D layered structure of **1** featuring OH···O hydrogen bonding (view along *c* axis). The $Me_3Si$ group and hydrogen atoms of $CH_2$ are omitted for clarity.

$(OEt)_2$ (**2a**), as the major product along with minor amounts of $Me_3SiCH(CH_3)P(O)(OEt)_2$ (~5%), which can be separated by column chromatography. The acid hydrolysis of the phosphonate esters **1a** and **2a** proceed under reflux conditions to afford the corresponding phosphonic acids **1** and **2** as white crystalline solids in nearly quantitative yield.

$$Me_3SiCR_2P(O)(OEt)_2 \xrightarrow[120^\circ C,30h]{\text{dilute HCl}} \underset{R = H(\mathbf{1}),\ CH_3(\mathbf{2})}{Me_3SiCR_2P(O)(OH)_2} + 2C_2H_5OH$$

For **1** and **2**, medium-intensity IR absorption at 2360 $cm^{-1}$ is suggestive of hydrogen bonded P–OH groups, while characteristic absorptions due to $\nu PO_3$ and $\nu Si–Me$ appear at 1205 and 1260 $cm^{-1}$, respectively. The $^1H$ and $^{13}C$ NMR spectra provide distinct $J_{P–H}$ and $J_{P–C}$ coupling information (Supporting Information, Figures S1 and S2) and establish the identity of each compound. In conformity with earlier reports,[15] electrospray ionization mass (ESI-MS) spectra (positive ion mode) reveal the existence of hydrogen bonded aggregates in solution along with the expected molecular ion peak at *m*/*z* 191.0276 $[M + Na]^+$ and 197.0747 $[M + H]^+$ for **1** and **2**, respectively.

Single crystals suitable for X-ray crystallography were grown from a solution of **1** and **2** separately in diethyl ether. The crystal data are summarized in Table 1, while selected bond lengths and angles are shown in Tables 2 and 3, respectively. The molecular structures (Figures 1 and 2) reveal that sterically demanding trimethylsilyl group imposes considerable strain, and this is reflected in wide Si–C–P bond angles [118.50(10)° (**1**); 112.63(8)° (**2**)], greater than the expected tetrahedral angle of 109.5°. In addition, elongation in the Si–C bond [1.8916(18) (**1**); 1.9226(16) Å (**2**)] also occurs to relieve the steric strain. These features are in conformity with structural studies of 1,3-disilapropane reported earlier.[16] The involvement of P–OH and P═O groups in OH···O hydrogen bonding extends the molecular structure of **1** into a layered motif featuring fused noncentrosymmetric 14-membered rings. On the other hand, the structure of **2** adopts a ribbonlike 1D motif, which is commonly observed in alkylphosphonic acids.[17] The O···O bond distance associated with hydrogen bonds in **1** and **2** lies in the range of 2.557–2.634 Å, whereas the hydrogen bond angles (O–H···O) vary between 165(4) and 176(2)°.

**Synthesis and Characterization of Diorganotin(IV) Coordination Polymers.** Following our earlier approach,[7]


dx.doi.org/10.1021/ic500682t | Inorg. Chem. 2014, 53, 6195–6203

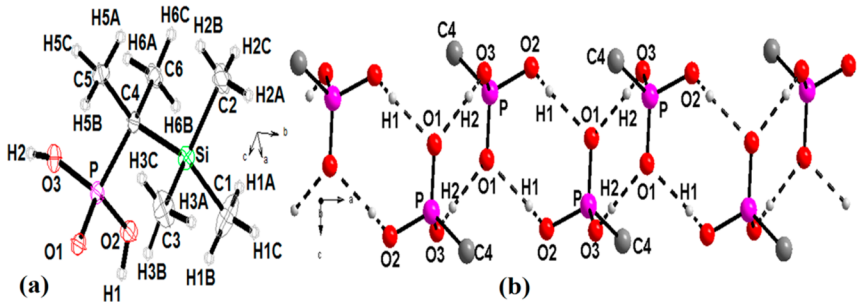


**Figure 2.** (a) ORTEP view of asymmetric unit of **2**. The thermal ellipsoids are set at 40% probability. (b) 1D ribbonlike structural motif of **2** showing O−H···O hydrogen bonding interactions (view along *b* axis). The $Me_3Si$ and $CH_3$ groups are omitted for clarity.

the reaction between equimolar quantities of diethyltin(methoxy)methanesulfonate $Et_2Sn(OMe)OSO_2Me$ and silaalkylphosphonic acid (**1** or **2**) proceeds under mild conditions ($CH_2Cl_2$, room temperature (rt), 8 h) to afford the isolation of $Et_2Sn\{OP(O)(OH)CH_2SiMe_3\}(OSO_2Me)$ (**3**) and $(Et_2Sn)_6\{O_3PC(CH_3)_2SiMe_3\}_4(OSO_2Me)_4$ (**4**). The chemoselective reactivity of Sn−OMe group in the precursor tin complex toward the phosphonic acids is in accord with more basic character of the methoxide group as compared to the alkanesulfonate group. The synthesis of $Et_2Sn(O_3PCH_2SiMe_3)$ (**5**) was achieved by azeotropic dehydration reaction between equimolar quantities of diethyltin oxide and phosphonic acid **1** in toluene under reflux conditions. The compounds **3**−**5** are obtained as white crystalline solids. While **3** and **4** are readily soluble in polar organic solvents such as methanol, dichloromethane, chloroform, etc., the solubility of **5** in hydrocarbon, aromatic, and ether solvents is quite unusual among this family of organotin(IV) phosphonates.

Single crystals suitable for X-ray crystallography were grown by diffusion of diethyl ether into a solution of **3** or **4** in methanol−chloroform mixture. The crystal data are summarized in Table 1, while selected bond lengths and angles are given in Tables 4 and 5, respectively. The structural motif of **3**

**Table 4. Selected Bond Lengths (Å) and Angles (deg) of 3**

| | | | |
|---|---|---|---|
| Sn−O(6)[a] | 2.1000(15) | Sn−C(3) | 2.122(2) |
| Sn−O(4) | 2.0987(14) | Sn−O(3)[b] | 2.5456(16) |
| Sn−O(1) | 2.4606(16) | Sn−C(1) | 2.112(2) |
| O(5)−H(5) | 0.830(17) | O(5)−H(5)···O(2)[c] | 2.632(2) |
| C3—Sn−C1 | 152.89(9) | O3[b]—Sn−O6[a] | 81.69(5) |
| O6[a]—Sn−O4 | 89.55(6) | O1—Sn−O4 | 84.18(6) |
| O3[b]—Sn−O1 | 104.57(6) | | |

[a]Symmetry transformations used to generate equivalent atoms: 2 − *x*, −*y*, 1 − *z*. [b]Symmetry transformations used to generate equivalent atoms: 1 − *x*, 1 − *y*, 1 − *z*. [c]Symmetry transformations used to generate equivalent atoms: 1 − *x*, −*y*, 1 − *z*.

represents 1D coordination polymer featuring alternate $[-Sn-O-P-O-]_2$ and $[-Sn-O-S-O-]_2$ eight-membered rings by virtue of bridging bidentate mode of both phosphonate and sulfonate ligands similar to that observed for analogous organotin complex $Et_2Sn\{OP(O)(OH)Ph\}(OSO_2Me)$, reported earlier.[7b] Thus, a more detailed discussion on the structural attributes is not warranted. The coordination assembly extends to a 2D motif (Figure 3b) as a result of hydrogen bonding interactions between uncoordinated oxygen atom O(2) of the sulfonate and P−OH groups [O5−H5 = 0.830(17), O5−H5···O2[iii] = 2.632(2) Å].

**Table 5. Selected Bond Lengths (Å) and Angles (deg) of 4**

| | | | |
|---|---|---|---|
| Sn1−O1 | 2.099(3) | Sn1−O4 | 2.094(3) |
| Sn1−O24[a] | 2.535(3) | Sn1−O20[b] | 2.549(3) |
| Sn1−C1 | 2.116(4) | Sn1−C3 | 2.117(5) |
| Sn2−O6 | 2.141(3) | Sn2−O13 | 2.276(3) |
| Sn2−O2 | 2.009(3) | Sn2−C7 | 2.121(5) |
| Sn2−C5 | 2.123(4) | Sn3−O5 | 2.025(3) |
| Sn3−O3 | 2.139(3) | Sn3−O16 | 2.320(3) |
| Sn3−C9 | 2.119(5) | Sn3−C11 | 2.127(4) |
| Sn4−O7 | 2.083(3) | Sn4−O10 | 2.125(3) |
| Sn4−O17 | 2.418(3) | Sn4−C13 | 2.110(4) |
| Sn4−C15 | 2.129(4) | Sn4−O14 | 2.623(3) |
| Sn5−O8 | 2.160(3) | Sn5−O11 | 2.015(3) |
| Sn5−O22 | 2.304(3) | Sn5−C17 | 2.136(4) |
| Sn5−C19 | 2.125(4) | Sn6−O12 | 2.134(3) |
| Sn6−O19 | 2.290(3) | Sn6−O9 | 2.008(3) |
| Sn6−C21 | 2.121(5) | Sn6−C23 | 2.129(5) |
| O24[a]−Sn1−O1 | 89.66(11) | O4−Sn1−O1 | 88.48(11) |
| O4−Sn1−O20[b] | 87.30(11) | O24[a]−Sn1−O20[b] | 94.54(12) |
| C3−Sn1−C1 | 157.48(18) | O−Sn2−C5 | 107.92(16) |
| O6−Sn2−O13 | 167.69(11) | C7−Sn2−C5 | 132.43(18) |
| C7−Sn2−O2 | 118.92(15) | O16−Sn3−O3 | 173.71(11) |
| C11−Sn3−C9 | 138.5(2) | O5−Sn3−C9 | 111.74(19) |
| O5−Sn3−C11 | 109.53(17) | O10−Sn4−O7 | 88.99(12) |
| O7−Sn4−O17 | 85.18(11) | O10−Sn4−O14 | 94.7(1) |
| O14−Sn4−O17 | 91.1(1) | C13−Sn4−C15 | 157.26(17) |
| O8−Sn5−O22 | 171.49(12) | O11−Sn5−C19 | 112.13(17) |
| O11−Sn5−C17 | 107.57(18) | C17−Sn5−C19 | 140.1(2) |
| O12−Sn6−O19 | 163.03(12) | O9−Sn6−C23 | 110.8(2) |
| O9−Sn−C21 | 114.15(17) | C21−Sn6−C23 | 134.6(2) |

[a] Symmetry transformations used to generate equivalent atoms: *x*, *y*, *z* − 1. [b] Symmetry transformations used to generate equivalent atoms: *x* + 1/2, −*y* + 1/2, *z* − 1/2.

The structure of **4** represents a hitherto unknown polymeric motif despite apparent similarity with respect to the presence of trinuclear tin phosphonate clusters with a $Sn_3P_2O_6$ core, which has been observed earlier in a few related examples in this family.[7a,e] The asymmetric unit is composed of a hexanuclear tin assembly of composition $[(Et_2Sn)_3(OSO_2Me)_2(O_3PR)_2]_2$ with two crystallographically unique trinuclear tin phosphonate clusters [Sn−O(P) = 2.008−2.160 Å] being associated with each other by the involvement of a methanesulfonate (S2) group [Sn3−O16(S2) = 2.320(3), Sn4−O17 = 2.418(3) Å]. The remaining sulfonate groups (S1, S3, and S4) perform in bridging bidentate fashion to drive the structure to a 2D coordination assembly in the *ac* plane (Figure 4). The tin atoms Sn2, Sn3, Sn5, and Sn6 in the layered structure adopt a distorted trigonal bipyramidal geometry with an $SnC_2O$


dx.doi.org/10.1021/ic500682t | Inorg. Chem. 2014, 53, 6195−6203

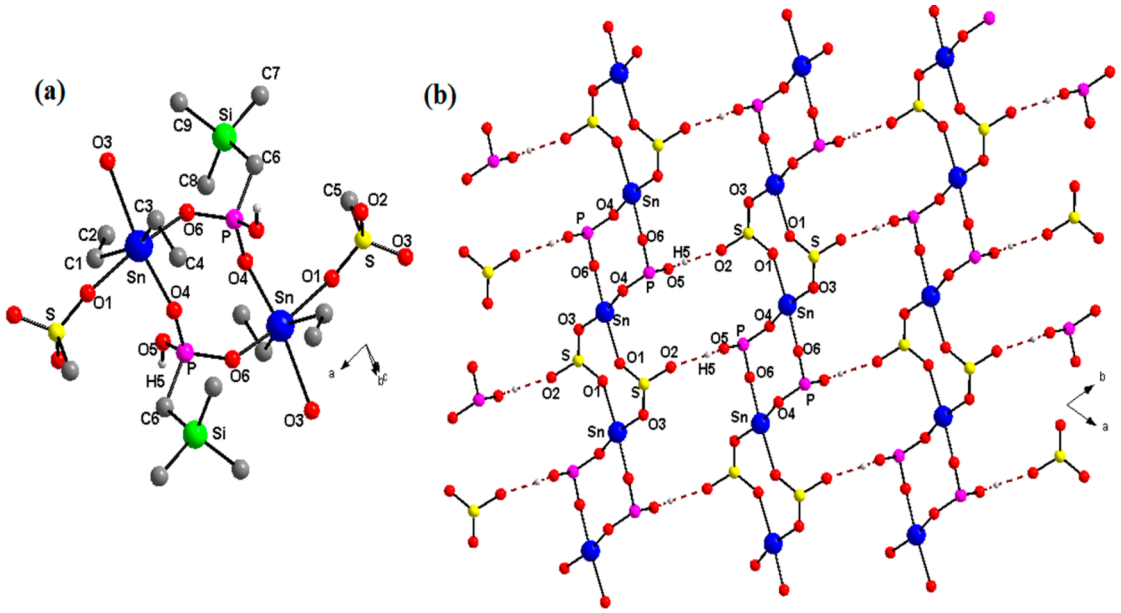


**Figure 3.** (a) Asymmetric unit of **3**. All the hydrogen atoms (except H5) are omitted for clarity. (b) 2D structural motif of **3** (view along *c* axis). The Si and all the carbon atoms are omitted for clarity. Hydrogen bonding interactions are shown by dashed lines.

equatorial atom set (Σ360 ± 0.2−0.73°), and the axial positions are occupied by oxygen atoms [∠O−Sn−O = 163.03(12)−173.71(11)°]. On the other hand, the tin atoms Sn1 and Sn4 adopt a distorted octahedral geometry with $SnO_4$ occupying the basal plane [Σ360 ± 0.02−0.03°] and trans position of ethyl groups [∠C−Sn−C = 157.26(17)−157.48(18)°]

**Spectroscopic Studies.** The identities of **3**−**5** were established by IR and multinuclear ($^1$H, $^{13}$C, $^{31}$P, $^{119}$Sn) NMR spectral studies, and the relevant data are summarized in the Experimental Section. For **3** and **4**, the observed IR absorptions in the region of 940−1200 cm$^{-1}$ are overlapping $\nu SO_3$ and $\nu PO_3$ stretching modes and, thus, are not informative in evaluating the coordination modes of these ligands. The $^{31}$P and $^{119}$Sn NMR spectra of **3** reveal a single resonance at $\delta$ 28.6 and −250, respectively. The lack of observed $^2J_{Sn-O-P}$ coupling suggests fluxional behavior of the compound in solution. However, the $^{119}$Sn NMR spectrum of **4** reveals a triplet centered at $\delta$ −237 ($^2J_{Sn-O-P}$ = 147.6 Hz) due to heteronuclear coupling with two neighboring phosphorus centers (see Supporting Information, Figure S3) and conforms to the presence of trinuclear tin phosphonate moiety in the structural framework as observed in solid state. For **5**, the $^{119}$Sn NMR spectral profile exhibits a quartetlike resonance centered around $\delta$ −282, while two distinct peaks at $\delta$ 17.1 (major) and 17.0 (minor) in the $^{31}$P NMR spectrum are flanked by partially resolved tin satellites of unequal intensity with $^2J_{Sn-O-P}$ coupling on the order of 141 Hz (Figure 5). These spectral attributes find a close analogy with those reported earlier for *n*-$Bu_2Sn(O_3PPh)$ by Biesemans et al.[2] On the basis of detailed NMR studies, it has been shown that each tin atom in the molecule is associated with three phosphonate groups. These results are in conformity with X-ray crystal structure of this compound, which adopts a 1D ladderlike structure by virtue of $\mu_3$-bonding mode of the phosphonate groups.[4a]

**Synthesis of Colloidal Particles from $Et_2Sn(O_3PCH_2SiMe_3)$ (5).** The preferential solubility of **5** in nonpolar solvents including hydrocarbons has interesting ramifications in miniaturization of the bulk sample by a wet chemical process. Thus, a solution of as-synthesized sample in ethanol−chloroform mixture (5:1) upon ultrasonication results in the formation of colloidal particles capable of scattering an incident laser light beam (Tyndall effect). The choice of solvent is found to be crucial since other combinations of solvents, such as methanol−chloroform, *n*-propanol−chloroform, and methanol−hexane, did not yield the desired effect. The morphology of colloidal particles was examined by scanning electron microscopy (SEM) and atomic force microscopy (AFM) studies. The SEM micrograph (Figure 6a) reveals that colloidal particles possess rodlike morphology, the largest dimension being on the order of 2 $\mu$m × 160 nm. A close view of the AFM image (tapping mode) shows that these colloidal particles are formed by aggregation of microcrystallites, and the height profile provides a dimension on the order of 40−60 nm (Figure 6b). The powder X-ray diffraction pattern of the sample obtained from the colloidal solution [see Supporting Information, Figure S4b] closely resembles that of the as-synthesized sample, suggesting structural integrity in the colloidal domain. Since the polymer **5** does not possess any functionality capable of forming hydrogen bonding interactions, it is reasonable to assume that bulk morphology of the as-synthesized sample in solid state (see Supporting Information, Figure S5) is predominately held by van der Waals interactions arising from silaalkyl chains, which can be depleted by proper choice of the solvent under sonicated conditions for which there exists enough precedence in literature.[18] In light of these results, we considered it appropriate to examine hydrolytic stability of **5** for possible applications. The bulk sample was kept in contact with deionized water for 24 h and was finally washed with acetone. The powder X-ray diffraction pattern of the dried sample remains essentially unchanged, with no new peak, and a little loss of intensity of lower 2$\theta$ values [see Supporting Information, Figure S4c].

## CONCLUSIONS

The silaalkylphosphonic acids **1** and **2** are shown to be potentially useful ligands in the isolation of diorganotin


dx.doi.org/10.1021/ic500682t | Inorg. Chem. 2014, 53, 6195−6203

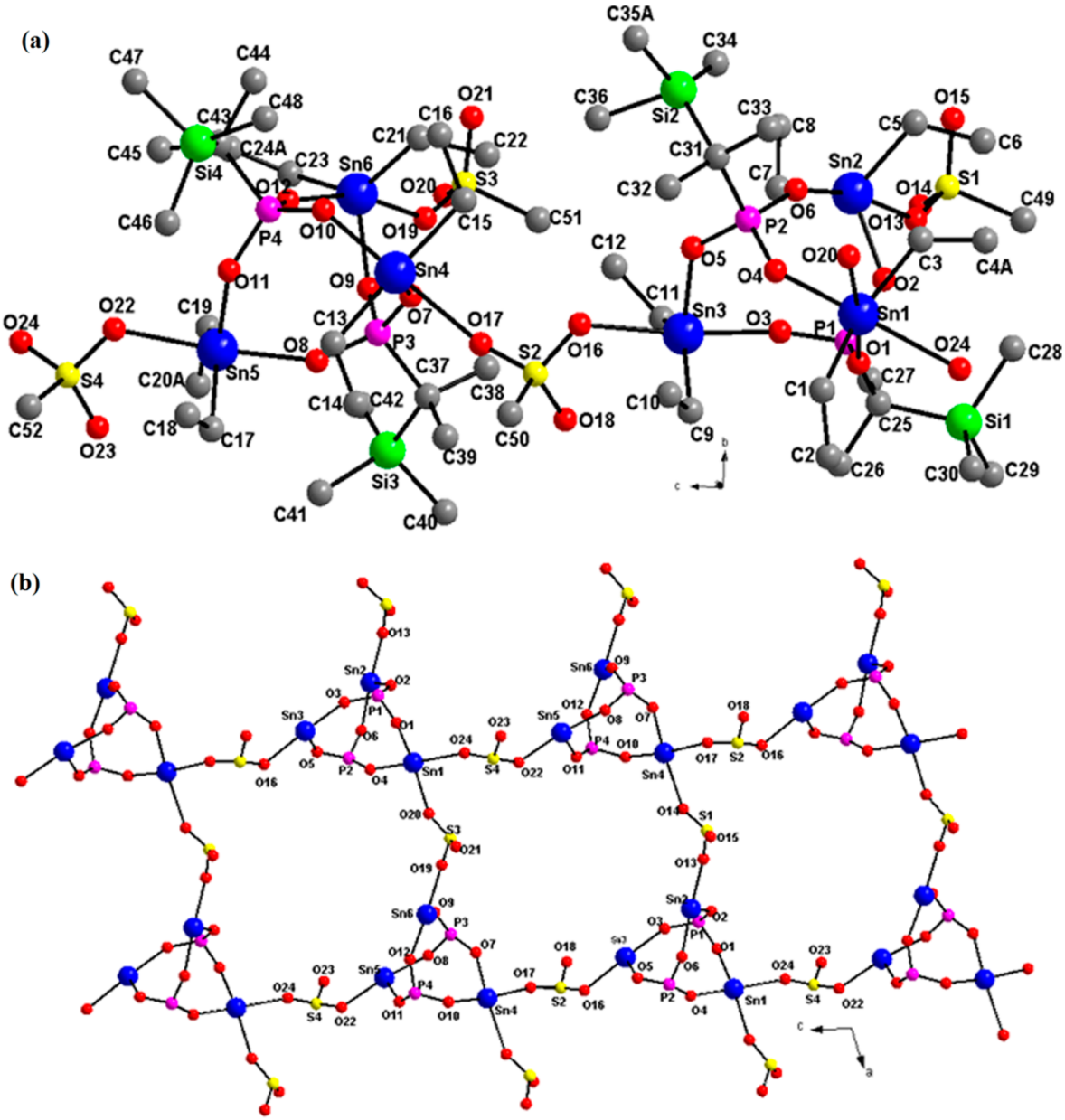


**Figure 4.** (a) Asymmetric unit of **4**. All the hydrogen atoms are omitted for clarity. (b) Extended 2D layered structure (view along *b* axis). The Si and all the carbon atoms are omitted for clarity.

coordination polymers with interesting structural motifs. The structural attributes of **3** and **4** are important additions to the family of stable mixed-ligand diorganotin coordination frameworks reported earlier from our group. For **5**, the presence of silaalkylphosphonate ligand significantly enhances the solubility in hydrocarbons, aromatics, and ether solvents. Taking advantage of this property, we have successfully utilized a wet chemical approach to achieve colloidal particles of **5** featuring rodlike morphology. Further studies are in progress to understand the properties associated with nano/colloidal sized organotin phosphonates.

## ■ EXPERIMENTAL SECTION

All operations were carried out using standard Schlenk line techniques under dry nitrogen atmosphere. Solvents were freshly distilled over phosphorus pentaoxide (dichloromethane and hexane) and over magnesium cake (methanol, ethanol). Glassware was dried in an oven at 110−120 °C and further flame-dried under vacuum prior to use. (Chloromethyl)trimethylsilane, triethylphosphite, *n*-butyl lithium (1.6 M in hexane), and methyl iodide (Aldrich) were used as supplied. Literature methods were used to prepare diethyltinoxide[19] and diethyltin(methoxy)methanesulfonate.[7e]

$^{1}$H, $^{13}$C{$^{1}$H}, $^{31}$P{$^{1}$H}, and $^{119}$Sn{$^{1}$H} NMR spectra were recorded on a BRUKER DPX-300 spectrometer at 300, 75.48, 121.50, and 119.92 MHz, respectively. $^{1}$H and $^{13}$C chemical shifts are quoted with respect to the residual protons of the solvents ($CDCl_3$), while $^{31}$P and $^{119}$Sn NMR data are given using 85% $H_3PO_4$ and tetramethyltin as the external standards, respectively. IR spectra were recorded on Nicolet protege 460 ESP spectrometer using KBr optics. Elemental analysis (C, H) was performed on a PerkinElmer model 2400 CHN elemental analyzer. The electron spray mass (ESI-MS) spectra were recorded using a Micromass Quattro II triple quadrupole mass spectrometer. The samples dissolved in chloroform−acetonitrile were introduced into the ESI source through a syringe pump at the rate of 5 L min$^{-1}$. The ESI capillary was set at 3.5 kV, and the cone voltage was 40 V. Phase determination was done by using the powder XRD technique


dx.doi.org/10.1021/ic500682t | *Inorg. Chem.* 2014, 53, 6195−6203

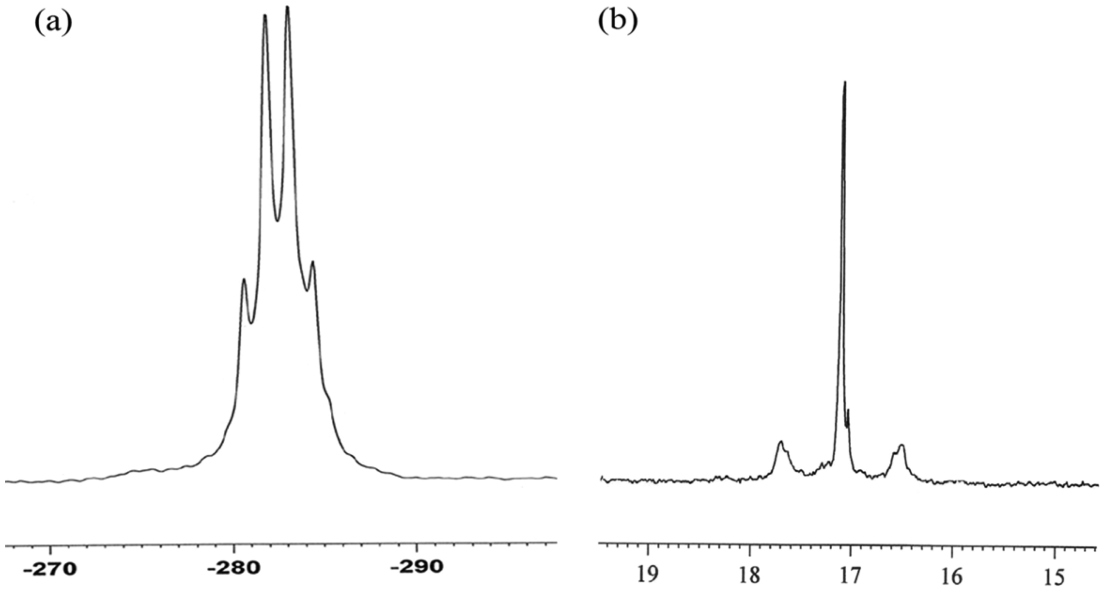


**Figure 5.** (a) $^{119}$Sn and (b) $^{31}$P NMR spectrum of $Et_2Sn(O_3PCH_2SiMe_3)$ (**5**).

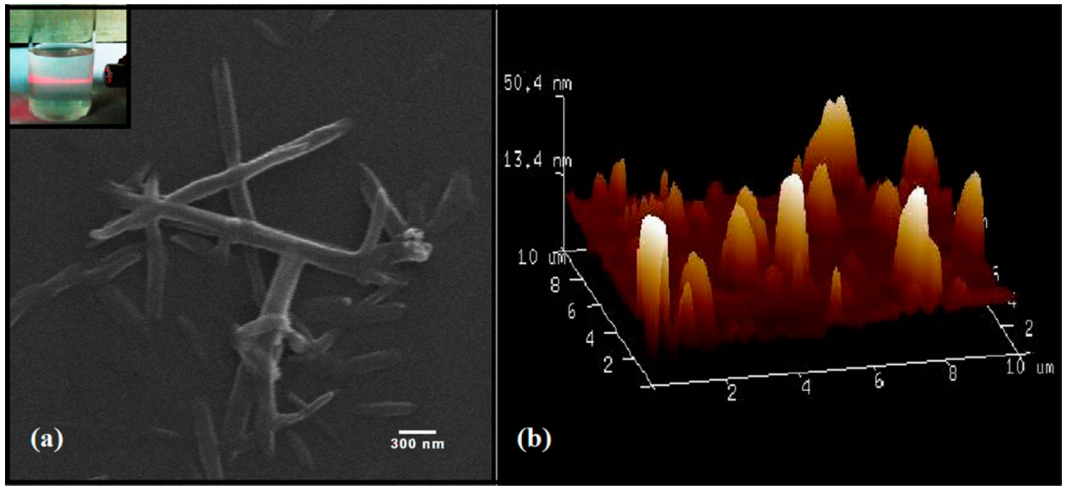


**Figure 6.** (a) SEM micrograph, (inset) demonstration of Tyndall effect, and (b) AFM image of **5**.

using Cu K$\alpha$ radiation on a Bruker D8 advance machine. A scanning electron microscope (SEM) EVO-50 from Carl Zeiss AG, Germany, was used to take images of the spin-coated samples. Tapping mode atomic force microscopy (AFM) was carried out on a Bruker Dimension Icon AFM. The images were acquired in air by using an MPP-11100−10 probe (Bruker; tip radius and resonance frequency are 8 nm and 75 kHz, respectively).

**Synthetic Methods.** *Synthesis of Trimethylsilylmethylphosphonic Acid (**1**).* Diethyltrimethylsilylmethylphosphonate **1a** was synthesized by following the known procedure[13a] using (chloromethyl)trimethylsilane (3.5 g, 28.66 mmol) and triethylphosphite (4.76 g, 28.66 mmol) as the reagents. The hydrolysis of **1a** (4.0 g) was performed using 120 mL of approximately 3 N HCl solution under refluxed conditions for 24−30 h. The product was extracted in diethyl ether and dried over sodium sulfate. The solution was concentrated and kept overnight under refrigeration to afford the isolation of **1** as white crystalline solid.

*$Me_3SiCH_2P(O)(OEt)_2$ (**1a**).* bp 120−122 °C/20 mm. Yield: 4.1 g, 65.0%. $^1$H NMR ($CDCl_3$): $\delta$ 4.03 (m, 4H, P−OC$H_2$), 1.29 (t, 6H, PO−$CH_2CH_3$, $^3J_{H-H}$ = 7.2 Hz), 1.12 (d, 2H, P−C$H_2$, $^2J_{P-H}$ = 21.9 Hz), 0.13 (S, 9H, Si−C$H_3$). $^{13}$C{$^1$H} NMR ($CDCl_3$): 60.9 (d, P−O−$CH_2$, $^2J_{P-O-C}$ = 6.3 Hz), 16.2 (d, P(OC$H_2$)$CH_3$, $^3J_{P-O-C}$ = 6.45 Hz), 14.4 (d, P−$CH_2$, $^1J_{P-C}$ = 127.65 Hz), −0.48 (S, Si−$CH_3$, $^1J_{Si-C}$ = 50.32 Hz). $^{31}$P{$^1$H} NMR ($CDCl_3$): $\delta$ 32.9. $^{29}$Si{$^1$H} NMR ($CDCl_3$): $\delta$ −0.19. Anal. Calcd for $C_8H_{21}O_3PSi$ (224.09): C, 42.84; H, 9.44. Found: C, 42.79; H, 9.52%.

*$Me_3SiCH_2P(O)(OH)_2$ (**1**).* Yield: 2.36 g, 79.0%. $^1$H NMR ($CDCl_3$): $\delta$ 7.95 (br, 2H, P−O*H*), 1.18 (d, 2H, P−C$H_2$, $^2J_{P-H}$ = 23.9 Hz), 0.16 (S, 9H, Si−C$H_3$). $^{13}$C{$^1$H} NMR ($CDCl_3$): 14.4 (d, P−$CH_2$, $^1J_{P-C}$ = 110.4 Hz), −0.51 (S, Si−$CH_3$). $^{31}$P {$^1$H} NMR ($CDCl_3$): $\delta$ 39.1. $^{29}$Si{$^1$H} NMR ($CDCl_3$): $\delta$ 0.13. IR (KBr, cm$^{-1}$): 1255 ($\nu_{Si-Me}$), 1198, 1132 ($\nu_{PO3}$), 2298 (br, $\nu_{P-OH}$), hydrogen bonded. ESI-MS ($m/z$): 191.0276 [M + Na]$^+$, 213.0095 [M−H + 2Na]$^+$, 381.0466 [2M−H + 2Na]$^+$, 403.0282 [2M−2H + 3Na]$^+$, 549.0835 [3M−H + 2Na]$^+$, 593.0479 [3M−3H + 4Na]$^+$, 739.1039 [4M−2H + 3Na]$^+$, 761.0855 [4M−3H + 4Na]$^+$. Anal. Calcd for $C_4H_{13}O_3PSi$ (168.04): C, 28.56; H, 7.79. Found: C, 28.51; H, 7.84%.

*Synthesis of (2-Trimethylsilyl)-2-propylphosphonic Acid (**2**).* To a solution of **1a** (5.0 g, 22.32 mmol) in dry THF was added 1.1 equiv of *n*-BuLi at −60 °C. After stirring for 3−4 h at rt, methyl iodide (1.5 equiv) was added at −60 °C, and the reaction mixture was stirred for 15 h at room temperature. The solution was poured into a saturated aqueous solution of $NH_4Cl$. The organic layer was separated, dried over sodium sulfate, and subjected to column chromatography over silica gel using a mixture of hexane and ethyl acetate (9:1) to afford the phosphonate diester **2a** as a colorless liquid. The transformation of **2a**


dx.doi.org/10.1021/ic500682t | *Inorg. Chem.* 2014, 53, 6195−6203

to the corresponding phosphonic acid **2** was achieved by following the procedure similar to that described above for **1**.

*$Me_3SiC(CH_3)_2P(O)(OEt)_2$ (**2a**).* bp 70−72 °C/0.07 mm. Yield: 3.9 g, 78.0%. $^1$H NMR ($CDCl_3$): $\delta$ 4.03 (m, 4H, P−OC$H_2$), 1.28 (t, 6H, PO−$CH_2CH_3$, $^3J_{H-H}$ = 7.2 Hz), 1.14 (d, 6H, P−C($CH_3$)$_2$, $^3J_{P-H}$ = 18.6 Hz), 0.08 (S, 9H, Si−$CH_3$). $^{13}$C{$^1$H} NMR ($CDCl_3$): 60.8 (d, P−$OCH_2$, $^2J_{P-O-C}$ = 6.15 Hz), 23.3 (d, P−$C(CH_3)$, $^1J_{P-C}$ = 134.8 Hz), 19.1 (d, P−$CH_2$, $^2J_{P-C}$ = 5.6 Hz), 16.3(d, P($OCH_2$)$CH_3$, $^3J_{P-O-C}$ = 6.5 Hz), −1.5 (S, Si−$CH_3$). $^{31}$P{$^1$H} NMR ($CDCl_3$): $\delta$ 38.4. $^{29}$Si{$^1$H} NMR ($CDCl_3$): $\delta$ −0.26. Anal. Calcd for $C_{10}H_{25}O_3PSi$ (252.13): C, 47.59; H, 9.99. Found: C, 47.53; H, 10.01%.

*$Me_3SiC(CH_3)_2P(O)(OH)_2$ (**2**).* Yield: 2.4 g, 77.0%. $^1$H NMR ($CDCl_3$): $\delta$ 7.40 (br, 2H, P−O*H*), 1.20 (d, 6H, P−C($CH_3$)$_2$, $^3J_{P-H}$ = 18.6 Hz), 0.14 (S, 9H, Si−$CH_3$). $^{13}$C{$^1$H} NMR ($CDCl_3$): 23.2 (d, P−C($CH_3$)$_2$, $^1J_{P-C}$ = 136.6 Hz), 19.1 (d, P−C($CH_3$)$_2$, $^2J_{P-C}$ = 5.6 Hz), −2.0 (S, Si−$CH_3$). $^{31}$P{$^1$H} NMR ($CDCl_3$): $\delta$ 45.2. $^{29}$Si{$^1$H} NMR ($CDCl_3$): $\delta$ 0.03. IR (KBr, cm$^{-1}$): 1251 ($\nu_{Si-Me}$), 1205, 1134 ($\nu_{PO3}$), 2358 (br, $\nu_{P-OH}$), hydrogen bonded. ESI-MS (*m*/*z*): 197.0747 [M + H]$^+$, 393.1427 [2M + H]$^+$, 589.2137 [3M + H]$^+$, 785.2891 [4M + H]$^+$, 981.3614 [5M + H]$^+$, 1177.4359 [6M + H]$^+$. Anal. Calcd for $C_6H_{17}O_3PSi$ (196.06): C, 36.72; H, 8.73. Found: C, 36.68; H, 8.81%.

*Synthesis of **3**−**5**.* The solution containing diethyltin(methoxy)-methanesulfonate (0.52 g, 1.74 mmol) and **1** (0.30 g, 1.74 mmol) or **2** (0.35 g, 1.74 mmol) in dichloromethane was stirred for 8 h at room temperature. Thereafter, the solvent was removed under vacuum, and *n*-hexane was added to afford, in each case, a white solid, which was filtered and dried under vacuum. The synthesis of **5** was achieved by azeotropic dehydration reaction between diethyltin oxide (0.52 g, 1.74 mmol) and **1** (0.30 g, 1.74 mmol) in toluene under refluxed conditions. The product was precipitated using methanol.

*$Et_2Sn\{OP(O)(OH)CH_2SiMe_3\}(OSO_2Me)$ (**3**).* Yield: 0.65 g, 88.0%. $^1$H NMR ($CDCl_3$): $\delta$ 2.77 (S, 3H, S$CH_3$), 1.66 (br, 4H, Sn$CH_2$), 1.34 (t, 6H, Sn($CH_2$)$CH_3$, $^3J_{H-H}$ = 8.1 Hz), 1.21 (d, 2H, P−$CH_2$, $^2J_{P-H}$ =12 Hz), 0.11 (S, 9H, Si−$CH_3$). $^{13}$C{$^1$H} NMR ($CDCl_3$): $\delta$ 39.3 (S, S−$CH_3$), 20.7 (S, Sn−$CH_2$, $^1J_{Sn-C}$ = 648 Hz), 17.3 (d, P−$CH_2$, $^1J_{P-C}$ = 129.7 Hz), 9.2 (S, Sn($CH_2$)$CH_3$, $^2J_{Sn-C}$ = 35.46 Hz), −0.26 (S, Si−$CH_3$). $^{31}$P{$^1$H} NMR ($CDCl_3$): $\delta$ 28.6. $^{119}$Sn{$^1$H} NMR ($CDCl_3$): $\delta$ −250. IR (KBr, cm$^{-1}$): 1208, 1194, 1118, 1057 ($\nu_{SO3}$ + $\nu_{PO3}$), 1240 ($\nu_{Si-Me}$), 2362 ($\nu_{P-OH}$), hydrogen bonded. Anal. Calcd for $C_9H_{25}O_6PSSiSn$ (439.99): C, 24.62; H, 5.74. Found: C, 24.54; H, 5.81%.

*$(Et_2Sn)_6\{O_3PC(CH_3)_2SiMe_3\}_4(OSO_2Me)_4$ (**4**).* Yield: 2.0 g, 54.0%. $^1$H NMR ($CDCl_3$): $\delta$ 2.80 (S, 3H, S$CH_3$), 1.74 (br, 4H, Sn−$CH_2$), 1.43 (t, 6H, Sn($CH_2$)$CH_3$, $^3J_{H-H}$ = 7.5 Hz), 1.18 (d, 6H, P−C($CH_3$)$_2$, $^3J_{P-H}$ = 19.2 Hz), 0.09 (S, 9H, Si−$CH_3$). $^{13}$C{$^1$H} NMR ($CDCl_3$): $\delta$ 39.6 (S, S−$CH_3$), 23.1 (d, P−$CH_2$, $^1J_{P-C}$ = 133.7 Hz), 20.4 (S, Sn−$CH_2$), 19.2 (d, P−C($CH_3$)$_2$, $^2J_{P-C}$ = 5.6 Hz), 9.4 (S, Sn($CH_2$)$CH_3$), −2.6 (S, Si−$CH_3$). $^{31}$P{$^1$H} NMR ($CDCl_3$): $\delta$ 31.6 ($^2J_{Sn-O-P}$ = 147.4 Hz). $^{119}$Sn{$^1$H} NMR ($CDCl_3$): $\delta$ −237 ($^2J_{Sn-O-P}$ = 147.6 Hz). IR (KBr, cm$^{-1}$): 1208, 1085, 1036, 1002 ($\nu_{SO3}$ + $\nu_{PO3}$), 1245 ($\nu_{Si-Me}$). Anal. Calcd for $C_{52}H_{132}O_{24}P_4S_4Si_4Sn_6$ (2218.19): C, 28.15; H, 6.00. Found: C, 28.09; H, 6.08%.

*$Et_2Sn(O_3PCH_2SiMe_3)$ (**5**).* Yield: 0.40 g, 68.0%. $^1$H NMR ($CDCl_3$): 1.66−1.64 (br, 4H, Sn−$CH_2$), 1.39−1.28 (br, 6H, Sn−$CH_3$), 1.00 (d, 2H, P−$CH_2$, $^2J_{P-H}$ = 21 Hz), 0.11 (S, 9H, Si−$CH_3$), $^{13}$C{$^1$H} NMR ($CDCl_3$): 21.1 (S, Sn−$CH_2$), 18.5 (d, P−$CH_2$, $^1J_{P-C}$ = 129.7 Hz), 9.9 (S, Sn($CH_2$)$CH_3$), 0.23 (S, Si−$CH_3$, $^3J_{P-C}$ = 3.7 Hz), $^{31}$P{$^1$H} NMR ($CDCl_3$): $\delta$ 17.1 ($^2J_{Sn-O-P}$ = 141 Hz). $^{119}$Sn{$^1$H} NMR ($CDCl_3$): −282 (q, $^2J_{Sn-O-P}$ = 141 Hz). IR (KBr, cm$^{-1}$): 1092, 1036, 1002 ($\nu_{PO3}$), 1260 ($\nu_{Si-Me}$). Anal. Calcd for $C_8H_{21}O_3PSiSn$ (344.00): C, 28.01; H, 6.17. Found: C, 27.98; H, 6.23%.

**X-ray Crystallography.** The intensity data of **1**−**4** were collected using a Nonius Kappa CCD diffractometer equipped with a molybdenum-sealed tube and a highly oriented graphite monochromator at 150(2) K. Cell parameters, data reduction, and absorption corrections were performed using Nonius software (DENZO and SCALEPACK).[20] The structure was solved by direct methods using SIR-97[21] and refined by a full-matrix least-squares method on $F^2$ using SHELXL-2013.[22] All calculations and graphics were performed using WinGx.[23] Partial atoms were refined isotropically. Frames were collected by $\omega$, $\varphi$, and 2$\theta$ rotation at 10 s per frame with SAINT.[24] The measured intensities were reduced to $F^2$ and corrected for absorption with SADABAS.[25] Structure solution, refinement, and data output were carried out using the SHELXTL program.[26] All the non-H atoms were refined anisotropically. H atoms were placed in geometrically calculated positions by using a riding model unless stated otherwise. Images were created using the Diamond program.[27] In compound **4**, one trimethylsilyl group is disordered over two sites in the ratio of 1:1, and three ethyl groups are disordered in the ratio of 2:1. The atom C24A in one disordered ethyl group was refined with restrained atomic displacement parameters (ADP).

## ■ ASSOCIATED CONTENT

### Ⓢ Supporting Information

Selected NMR spectra, powder X-ray diffraction pattern, scanning electron micrograph, and crystallographic data for the structural analysis (in CIF format). This material is available free of charge via the Internet at http://pubs.acs.org. Related crystallographic information can be obtained free of charge from the CCDC via www.ccdc.cam.ac.uk/data_request/cif (CCDC Nos. 991294−991297 for **1**−**4**).

## ■ AUTHOR INFORMATION


### Corresponding Author

*E-mail: shankar@chemistry.iitd.ac.in.


### Notes

The authors declare no competing financial interest.

## ■ ACKNOWLEDGMENTS


The work was supported by CSIR Grant No. [01(2651)/12/EMR-II]. N.S. is grateful to CSIR for providing Senior Research Fellowship.


## ■ REFERENCES


(1) (a) Song, S.-Y.; Ma, J.-F.; Yang, J.; Gao, L.-L.; Su, Z.-M. *Organometallics* **2007**, *26*, 2125. (b) Kumara Swamy, K. C.; Schmid, C. G.; Day, R. O.; Holmes, R. R. *J. Am. Chem. Soc.* **1990**, *112*, 223. (c) Chandrasekhar, V.; Baskar, V.; Steiner, A.; Zacchini, S. *Organometallics* **2002**, *21*, 4528.

(2) Ribot, F.; Sanchez, C.; Biesemans, M.; Mercier, F. A. G.; Martins, J. C.; Gielen, M.; Willem, R. *Organometallics* **2001**, *20*, 2593.

(3) Molloy, K. C.; Hossain, M. B.; van der Helm, D.; Cunningham, D.; Zuckerman, J. *J. Inorg. Chem.* **1981**, *20*, 2402.

(4) (a) Xie, Y.-P.; Ma, J.-F.; Yang, J.; Su, M.-Z. *Dalton Trans.* **2010**, *39*, 1568. (b) Ma, C.; Yang, M.; Zhang, R.; Du, L. *Inorg. Chim. Acta* **2008**, *361*, 2979.

(5) Molloy, K. C.; Nasser, F. A. K.; Barnes, C. L.; Helm, D. V. D.; Zuckerman, J. *J. Inorg. Chem.* **1982**, *21*, 960.

(6) (a) Mehring, M.; Löw, C.; Schürmann, M.; Jurkschat, K. *Eur. J. Inorg. Chem.* **1999**, 887. (b) Mehring, M.; Vrasidas, I.; Horn, D.; Schürmann, M.; Jurkschat, K. *Organometallics* **2001**, *20*, 4647. (c) Peveling, K.; Henn, M.; Löw, C.; Mehring, M.; Schürmann, M.; Costisella, B.; Jurkschat, K. *Organometallics* **2004**, *23*, 1501.

(7) (a) Shankar, R.; Jain, A.; Kociok-Köhn, G.; Molloy, K. C. *Inorg. Chem.* **2011**, *50*, 1339. (b) Shankar, R.; Singh, A. P.; Jain, A.; Mahon, M. F.; Molloy, K. C. *Inorg. Chem.* **2008**, *47*, 5930. (c) Shankar, R.; Jain, A.; Singh, A. P.; Molloy, K. C. *Phosphorus, Sulfur Silicon Relat. Elem.* **2011**, *186*, 1375. (d) Shankar, R.; Singh, A. P.; Upreti, S. *Inorg. Chem.* **2006**, *45*, 9166. (e) Shankar, R.; Jain, A.; Singh, A. P.; Kociok-Köhn, G.; Molloy, K. C. *Inorg. Chem.* **2009**, *48*, 3608.

(8) (a) Spokoyny, A. M.; Kim, D.; Sumrein, A.; Mirkin, C. A. *Chem. Soc. Rev.* **2009**, *38*, 1218. (b) Oh, M.; Mirkin, C. A. *Nature Lett.* **2005**, *438*, 651. (c) Flügel, E. A.; Ranft, A.; Haase, F.; Lotsch, B. V. *J. Mater. Chem.* **2012**, *22*, 10119. (d) Xu, G.; Yamada, T.; Otsubo, K.; Sakaida, S.; Kitagawa, H. *J. Am. Chem. Soc.* **2012**, *134*, 16524.

(9) (a) Mas-Ballesté, R.; Gómez-Herrero, J.; Zamora, F. *Chem. Soc. Rev.* **2010**, *39*, 4220. (b) García-Couceiro, U.; Olea, D.; Castillo, O.; Luque, A.; Román, P.; Pablo, P. J. d.; Gómez-Herrero, J.; Zamora, F. *Inorg. Chem.* **2005**, *44*, 8343. (c) Amo-Ochoa, P.; Rodríguez-Tapiador, M. I.; Castillo, O.; Olea, D.; Guijarro, A.; Alexandre, S. S.; Gómez-Herrero, J.; Zamora, F. *Inorg. Chem.* **2006**, *45*, 7642. (d) Mateo-Martí, E.; Welte, L.; Amo-Ochoa, P.; Sanz Miguel, P. J.; Gómez-Herrero, J.; Martín-Gagoad, J. A.; Zamora, F. *Chem. Commun.* **2008**, 945.

(10) (a) Li, P.-Z.; Maeda, Y.; Xu, Q. *Chem. Commun.* **2011**, *47*, 8436. (b) Ochoa, P.-O.; Welte, L.; González-Prieto, R.; Sanz Miguel, P. J.; Gómez-Garcí, C. J.; Mateo-Martí, E.; Delgado, S.; Gómez-Herrero, J.; Zamora, F. *Chem. Commun.* **2010**, *46*, 3262. (c) Kondo, A.; Tiew, C. C.; Moriguchi, F.; Maeda, K. *Dalton Trans.* **2013**, *42*, 15267. (d) Tan, J.-C.; Saines, P. J.; Bithell, E. G.; Cheetham, A. K. *ACS Nano* **2012**, *6*, 615.

(11) Araki, T.; Kondo, A.; Maeda, K. *Chem. Commun.* **2013**, *49*, 552.

(12) (a) Clearfield, A. *Dalton Trans.* **2008**, 6089. (b) Subbiah, A.; Pyle, D.; Rowland, A.; Huang, J.; Narayanan, R. A.; Thiyagarajan, P.; Zoń, J.; Clearfield, A. *J. Am. Chem. Soc.* **2005**, *127*, 10826.

(13) (a) Canavan, A. E.; Eaborn, C. *J. Chem. Soc., Dalton Trans.* **1959**, 3751. (b) Keeber, W. H.; Howard, W. P. *J. Org. Chem.* **1956**, *21*, 509.

(14) Shankar, R.; Asija, M.; Singla, N.; Basu, S.; Kociok-Köhn, G.; Molloy, K. C. *Dalton Trans.* **2013**, *42*, 15591.

(15) (a) Mehring, M.; Schürmann, M.; Ludwig, R. *Chem.—Eur. J.* **2003**, *9*, 837. (b) Murugavel, R.; Singh, M. P. *New J. Chem.* **2010**, *34*, 1846.

(16) (a) Shankar, R.; Joshi, A.; Upreti, S. *Polyhedron* **2006**, *25*, 2183. (b) Fjeldberg, T.; Seip, R.; Lappert, M. F.; Thorne, A. J. *J. Mol. Str.* **1983**, *99*, 295. (c) Glidewell, C.; Liles, D. C. *J. Organomet. Chem.* **1982**, *234*, 15. (d) Almenningen, A.; Seip, H. M.; Seip, R. *Acta Chem. Scand.* **1970**, *24*, 1697.

(17) (a) Langley, K. J.; Squattrito, P. J.; Adani, F.; Montoneri, E. *Inorg. Chim. Acta* **1996**, *253*, 77. (b) Peterson, S. W.; Gebert, E.; Reis, A. H., Jr.; Druyan, M. E.; Mason, G. W.; Peppard, D. F. *J. Phys. Chem.* **1977**, *81*, 466. (c) Uchtman, V. A.; Gloss, R. A. *J. Phys. Chem.* **1972**, *76*, 1298. (d) DeLaMatter, D.; McCullough, J. J.; Calvo, C. *J. Phys. Chem.* **1973**, *77*, 1146.

(18) (a) Wong, M.; Ishige, R.; Hoshino, T.; Hawkins, S.; Li, P.; Takahara, A.; Sue, H.-J. *Chem. Mater.* **2014**, *26*, 1528.

(19) Ingham, R. K.; Rosenberg, S. D.; Gilman, H. *Chem. Rev.* **1960**, *60*, 459.

(20) Otwinowski, Z.; Minor, W. Processing of X-ray Diffraction Data Collected in Oscillation Mode. In *Methods in Enzymology,* Vol. *276*: Macromolecular Crystallography, Part A; Carter, C. W., Jr., Sweet, R. M., Eds.; Academic Press: San Diego, CA, 1997; p 307, HKL DENZO and SCALE-PACK, version 1.96.

(21) Altormare, A.; Burla, M. C.; Carnalli, M.; Cascarano, G.; Giacovazzo, C.; Guagliardi, A.; Moliterni, A. G. G.; Polidori, G.; Spagan, R. *J. Appl. Crystallogr.* **1999**, *32*, 115.

(22) Sheldrick, G. M. *Acta Crystallogr., Sect. A: Fundam. Crystallogr.* **2008**, *64*, 112.

(23) Farrugia, L. J. *J. Appl. Crystallogr.* **1999**, *32*, 837.

(24) *SMART: Bruker Molecular Analysis Research Tool,* Version 5.618; Bruker AXS: Madison, WI, 2000.

(25) *SAINT-NT,* Version 6.04; Bruker AXS: Madison, WI, 2001.

(26) *SHELXTL-NT,* Version 6.10; Bruker AXS: Madison, WI, 2000.

(27) Klaus, B. *DIAMOND,* Version 1.2c; University of Bonn: Bonn, Germany, 1999.